

# Electron-phonon interaction contribution to the total energy of group IV semiconductor polytypes

R. Arjun Varma,<sup>1</sup> Shilpa Paul,<sup>1</sup> Anup Itale,<sup>1</sup> Pranav Pable,<sup>1</sup> Radhika Tibrewala,<sup>1</sup> Samruddhi Dodal,<sup>1</sup> Harshal Yerunkar,<sup>1</sup> Saurav Bhaumik,<sup>2</sup> Vaishali Shah,<sup>3</sup> M. P. Gururajan,<sup>1</sup> and T. R. S. Prasanna<sup>1,\*</sup>

<sup>1</sup>*Department of Metallurgical Engineering and Materials Science,  
Indian Institute of Technology Bombay, Mumbai 400076, India*

<sup>2</sup>*Department of Mathematics, Indian Institute of Technology Bombay, Mumbai 400076, India*

<sup>3</sup>*Department of Scientific Computing, Modeling and Simulation,  
Savitribai Phule Pune University, Pune 411007, India*

(Dated: April 19, 2022)

In density functional theory (DFT) based total energy studies, the van der Waals (vdW) dispersion and zero-point vibrational energy (ZPVE) correction terms are included to obtain energy differences between polymorphs. We introduce a new correction term, due to electron-phonon interactions (EPI). We calculate EPI corrections to the total energy for cubic and hexagonal polytypes of Carbon, Silicon and Silicon Carbide. The EPI corrections alter the energy differences between polytypes in C, Si, and SiC; especially in C and SiC where the EPI strength is significant. The EPI correction term is more sensitive to crystal structure than the vdW and ZPVE terms in SiC polytypes making it more important in determining energy differences. Including EPI corrections establishes that, in *ab initio* studies, the cubic SiC-3C is metastable and hexagonal SiC-4H is the stable polytype. For these studies, we extend Allen's formalism and this enables, for the first time, inclusion of EPI corrections as separate terms in the free energy expression. This opens the way to study their role on all thermodynamic properties through the Quasi-Harmonic Approximation.

The group IV semiconductors, especially C, Si and SiC, are of immense scientific and technological importance. Currently, there is enormous interest in predicting new allotropes of C and Si because different crystal structures exhibit differing physical properties and provide a landscape to design materials with specific properties [1–5]. In the case of C, this is evident from the 522 allotropes listed in the Samara Carbon allotrope database [6]. In Si, predicting metastable crystal structures with direct band-gaps are of interest [7]. SiC polytypes are among the most important materials for structural applications [8]. SiC also has promising potential in future high-voltage and low-loss power devices [9].

Given their importance, several studies have been performed on C, Si and SiC polymorphs. The accurate determination of the energy differences is essential to the study of these polymorphs. There is disagreement between DFT and experimental studies on the stable SiC polytype [10–15]. Experiments suggest that the cubic SiC-3C is stable at lower temperatures [12–15]. However, DFT studies have consistently shown that the hexagonal SiC-6H and SiC-4H are more stable than cubic SiC-3C [10–15]. To resolve this discrepancy, Heine et al. [14, 15] have proposed an explanation for the preference of SiC to grow in the metastable SiC-3C crystal structure.

Studies incorporating the van der Waals (vdW) dispersion correction in density-functional theory (DFT) calculations show SiC-3C is the stable polytype [12, 13]. Recently, for materials where polymorphs differ marginally in energy (SiC, BN, B, Fe<sub>2</sub>P etc.), the stable polymorphs have been determined by including the vdW dispersion and the zero-point vibrational energy (ZPVE) correc-

tions. Including these corrections frequently alters the polymorph stability order [12, 13, 16–19].

However, these studies do not consider the contributions from electron-phonon interactions (EPI). Electron-phonon interactions have been well studied for their role in several electronic and optical properties [20, 21]. In semiconductors and insulators, the experimental observation of the temperature dependence of band gaps is explained by the temperature dependence of eigenenergies,  $E_{n\mathbf{k}}(T)$  [20, 21]. Since the total energy is related to  $E_{n\mathbf{k}}(T)$ , the role of EPI in total energy and other thermodynamic properties must be studied.

In this paper, we introduce, for the first time, EPI corrections to the total energy. It alters the energy differences between polytypes in C, Si and SiC. For SiC polytypes, the EPI term is more important, compared to the ZPVE and the vdW dispersion terms, in determining relative stability. It clearly establishes the metastability of the cubic SiC-3C polytype in *ab initio* studies. For these studies, we extend Allen's formalism and this enables, for the first time, inclusion of EPI corrections as separate terms in the free energy expression. This opens the way to study their role on all thermodynamic properties through the Quasi-Harmonic Approximation (QHA).

In the Allen-Heine theory [22–26], electron-phonon interactions lead to contributions from the Fan-Migdal (FM) [27, 28] and the Debye-Waller (DW) [29] terms to the eigenenergies. The temperature dependent eigenenergies are given by  $E_{n\mathbf{k}}(T) = \epsilon_{n\mathbf{k}} + \Delta\epsilon_{n\mathbf{k}}(T)$  where  $\epsilon_{n\mathbf{k}}$  is the static lattice eigenenergy for wave vector  $\mathbf{k}$  and band  $n$  and the EPI correction is given by  $\Delta\epsilon_{n\mathbf{k}}(T) = \Delta^{FM}\epsilon_{n\mathbf{k}}(T) + \Delta^{DW}\epsilon_{n\mathbf{k}}(T)$ . Due to the presence of zero-

point vibrations, the zero-point renormalization (ZPR) of electron eigenenergies,  $\Delta\epsilon_{n\mathbf{k}}(0)$ , has finite values.

In free energy studies, we extend Allen's formalism [43] for including the renormalization of eigenenergies of electrons and phonons (due to interactions) in the QHA. The electron eigenenergy is given by

$$\epsilon_K^{QP}(V, T) = \epsilon_K(V_0) + \Delta\epsilon_K^{QH} + \Delta\epsilon_K^{QP}(V, T) \quad (1)$$

The first term is the eigenenergy for static lattice parameters. The second term is the change when vibrational free energy is included to determine the equilibrium lattice parameters. The third term is the contribution of interactions (e.g. EPI).

When the eigenenergy contains only the first two terms of Eq. 1, the free energy expression for non-interacting particles is used. Including the third term requires another method to calculate the free energy. The difference in free energies between the two methods is the free energy contribution due to interactions (e.g. EPI).

For the energy term, the main difference is the inclusion of the third term,  $\Delta_{ep}\epsilon_K^{QP}(V, T)$ , in the second method. Thus, summing over occupied states gives the EPI correction to the (total) energy which is also the EPI correction to the band-structure energy and given by

$$\Delta E_{av}^{ep}(V, T) = \sum_K^{occ} \Delta_{ep}\epsilon_K^{QP}(V, T) \quad (2)$$

The contribution from the entropy term is zero in both methods in semiconductors and insulators. Thus, the EPI contribution to the free energy is the EPI contribution to the total energy

$$\Delta F_{epi}(V, T) = \Delta E_{av}^{ep}(V, T) = 2 \sum_{n, \mathbf{k}}^{occ, IBZ} w_{\mathbf{k}} \Delta\epsilon_{n\mathbf{k}}(V, T) \quad (3)$$

In metals, additional terms are present in both methods. They mostly affect the entropy contributions. Thus, Eq.2 is also the main energy correction term in metals. (see Supplementary Information.)

Thus, Eq. 2 is valid for all classes of materials - metals, semiconductors and insulators. Since it does not depend on the EPI calculation method, it is applicable to results from Allen-Heine theory, *ab initio* molecular dynamics (AIMD) and other methods.

The extension of Allen's formalism makes it possible, for the first time, to include the EPI contributions as separate terms in the free energy expression.

In an AIMD study, Asker et al. [44] conclude that the temperature dependent energy differences between bcc and fcc Mo is due to the temperature dependent electronic density of states (EDOS). The smoothening of the sharp features of EDOS has been attributed to

adiabatic EPI [45]. It is clear that EPI causes the EDOS and hence, the band-structure energy to be temperature dependent, which in turn becomes the main reason for the total energy to be temperature dependent. Thus, the above study provides supporting evidence for Eq. 2. Indeed, Eq. 2 is the theoretical basis for the results. (See Supplementary Information.)

However, for semiconductors and insulators, instead of AIMD, the Allen-Heine theory can be used. It allows the calculation of EPI corrections to any arbitrary eigenstate,  $\Delta\epsilon_{n\mathbf{k}}(T)$ , including for the valence band maxima (VBM) and the conduction band minima (CBM). For this reason, it is the most widely used *ab initio* method in EPI studies of band gaps and band structures [30–42].

Thus, we can also obtain the EPI correction to the  $\mathbf{k}$ -points in the irreducible Brillouin zone (IBZ) that contribute to the DFT total energy. This allows the EPI corrections to the total energy (Eq. 2) to be calculated.

For IR-active materials, the non-adiabatic approximation must be used [34]. In this case, the ZPR shift,  $\Delta\epsilon_{n\mathbf{k}}(T)$ , varies linearly with  $1/N_q$ , where  $N_q^3$  is the total number of  $\mathbf{q}$ -points in the BZ [34, 41]. It follows from the linearity property of Eq. 3 that  $\Delta E_{av}^{ep}(T)$  will vary linearly with  $1/N_q$  (Proof in Supplementary Information).

In this study, we calculate the EPI correction to the total energy for the cubic and hexagonal polytypes of C, Si and SiC. All calculations were performed using the ABINIT software package [46–48] that has been used in several ZPR band-gap studies [33, 38–42].

For SiC polymorphs, the dispersion correction (DFT-D2 and DFT-D3(BJ)) [49, 50] was also applied to calculate the total energies and lattice parameters. An advantage of DFT-D methods is that the dispersion and EPI corrections are both incorporated by calculating the EPI corrections at the altered lattice parameters [40, 51].

We present results obtained for the ONCV pseudopotentials with PBE exchange-correlation functional. Similar results were obtained for other pseudopotentials. (See Supplementary Information). The energy cutoffs used were 30 Ha (Si) and 50 Ha (C and SiC). For hexagonal structures, the Broyden-Fletcher-Goldfarb-Shanno (BFGS) algorithm was used for structural optimization [46, 47]. An unshifted  $8 \times 8 \times 8$   $\mathbf{k}$ -point grid was used for cubic structures. For all hexagonal structures (except for SiC-4H for which  $9 \times 9 \times 3$   $\mathbf{k}$ -point grid was used), an unshifted  $9 \times 9 \times 5$   $\mathbf{k}$ -point grid was used.

The module on temperature dependence of the electronic structure was used for EPI calculations [48]. We provide the list of  $\mathbf{k}$ -points in the IBZ and additional  $\mathbf{k}$ -points corresponding to CBM. The  $\mathbf{q}$ -point grids were increased by 200-300  $\mathbf{q}$ -points in IBZ. To accelerate convergence, an imaginary smearing parameter,  $i\delta$ , of 100 meV and 50 meV was used [34, 40, 48]. The optimized number of bands used was 30 for SiC-4H and 22 for all other C, Si and SiC polymorphs. EPI corrections for SiC-6H could not be calculated due to computational constraints.

For C-dia, the ZPR of VBM, CBM and the lowest CB at  $\Gamma$ -point are 142 meV, -151.4 meV and -272.5 meV respectively. For Si-dia they are 34.27 meV, -21.24 meV and -8 meV respectively. These values are similar to the reported values [48]. The ZPR for other eigenstates in the IBZ were obtained in the same run.

Table I gives the lattice parameters, band gaps and the relative energy stability with and without EPI corrections for the C and Si polymorphs. Our DFT lattice parameters and relative stability energies are similar to those in literature [2, 52, 53]. Figure 1 shows the conver-

TABLE I. The lattice parameters, band gaps and energy differences for carbon and silicon polytypes. The unit for relative stability  $\Delta E$  is meV/atom

Material	a, c (Bohr)	Band gaps (Indirect/ Direct) (eV)	$\Delta E$	
			(DFT)	(DFT+EPI)
C-dia	6.75	4.18, 5.61	0	0
C-hex	4.75, 7.90	3.40, 5.01	24.3	67.9
Si-dia	10.34	0.61, 2.55	0	0
Si-hex	7.28, 12.03	0.45, 0.98	9.7	17.3

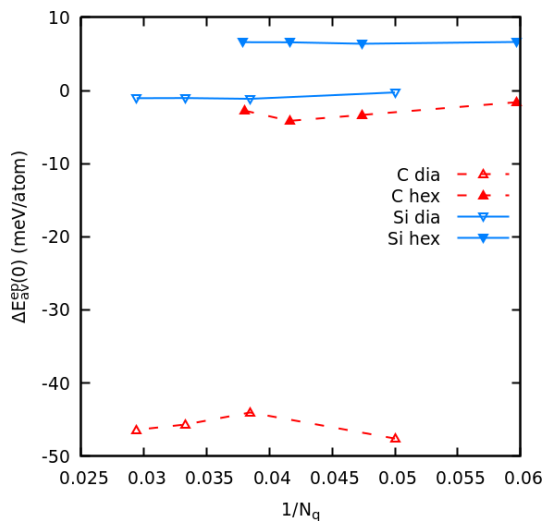


FIG. 1. Convergence of EPI correction to total energy with  $\mathbf{q}$ -point grid density (adiabatic approximation) for a smearing parameter of 100 meV for Carbon and Silicon polytypes.

gence behavior of  $\Delta E_{av}^{ep}(0)$  with  $1/N_q$  for  $i\delta = 100$  meV. Carbon/silicon polytypes show strong/weak EPI corrections consistent with the weaker electron-phonon interaction in silicon compared to carbon [31–40]. The negative value of  $\Delta E_{av}^{ep}(0)$  for C-dia implies that, averaged over the BZ, the Fan-Migdal term dominates over the DW term. In contrast to C-dia, a small value of  $\Delta E_{av}^{ep}(0)$  is obtained for C-hex. However, the ZPR of VBM, CBM and the lowest CB at  $\Gamma$ -point for C-hex are 117 meV, -172.6 meV and -313.9 meV respectively. They are com-

parable to those for C-dia indicating a strong electron-phonon interaction in C-hex. Thus, the small value of  $\Delta E_{av}^{ep}(0)$  in C-hex indicates a near balance between the FM and DW terms when averaged over the BZ.

Table I shows that including EPI corrections in *ab initio* studies of relative stability of allotropes is essential. After including EPI corrections the C-dia structure is more stable than the C-hex structure by  $\approx 68$  meV/atom compared to  $\approx 24$  meV/atom from DFT studies [2, 52, 53]. The Si-dia stability also increases from  $\approx 10$  meV/atom to  $\approx 17$  meV/atom.

Table II shows the lattice parameters, ZPR and the energy stabilities relative to the SiC-3C polytype. The indirect/direct band gaps (at the  $\Gamma$ -point) are 1.41 eV/6.13 eV (SiC-3C), 2.32 eV/4.72 eV (SiC-2H), 2.26 eV/5.01 eV (SiC-4H) and 2.07 eV/5.10 eV (SiC-6H). These results are very similar to literature values [10–13].

TABLE II. Lattice parameters, ZPR and energy stability of SiC polytypes relative to SiC-3C for DFT, DFT-D2 and DFT-D3(BJ) calculations.

Polytype	a, c (Bohr)	ZPR(meV) VBM/CBM	$\Delta E$ (meV/f.u.)
<b>3C-SiC</b>			
DFT	8.28	93.6/-56.3	0
DFT-D2	8.23	-	0
DFT-D3(BJ)	8.21	95.4/-55.6	0
<b>4H-SiC</b>			
DFT	5.85, 19.14	84.7/-61.3	-2.15
DFT-D2	5.81, 19.06	-	2.31
DFT-D3(BJ)	5.80, 18.99	86.3/-60.8	-1.81
<b>2H-SiC</b>			
DFT	5.84, 9.59	78.6/-88.9	5.07
DFT-D2	5.81, 9.56	-	14.2
DFT-D3(BJ)	5.80, 9.52	80.0/-86.5	6.32

In our DFT results, SiC-4H is more stable than SiC-3C similar to previous studies [10–13]. Including the DFT-D2 approximation makes SiC-3C to be the stable polytype, similar to recent studies [12, 13]. However, including the DFT-D3(BJ) approximation retains the DFT stability order where SiC-3C is metastable.

The ZPR of VBM/CBM for SiC-3C (obtained using parameters similar to those used in other studies [40]) is comparable to reported values [42].

Figure 2 shows the convergence behavior of  $\Delta E_{av}^{ep}(0)$  and a strong crystal structure dependence is evident. The  $\Delta E_{av}^{ep}(0)$  for SiC-4H (50% hexagonality) [12, 13] does not lie between the values for SiC-3C (0% hexagonality) and SiC-2H (100% hexagonality). A similar trend is also seen for DFT total energies (Table II and Ref. [10–13]).

Table III shows the stability of SiC-polytypes obtained by combining the EPI corrections to total energy in Figure 2 with the relative stability data in Table II. For SiC-3C and SiC-2H we consider  $\Delta E_{av}^{ep}(0)$  for the smallest value of  $1/N_q$ . However, for SiC-4H, the  $\Delta E_{av}^{ep}(0)$

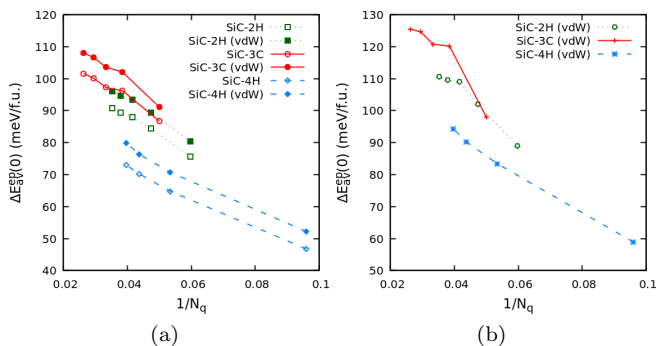


FIG. 2. Convergence of EPI correction to total energy with  $\mathbf{q}$ -point grid density (non-adiabatic approximation) for smearing parameters: a) 100 meV and b) 50 meV, for SiC polytypes for DFT and DFT-D3(BJ) lattice parameters.

varies by  $\lesssim 3$  meV/f.u. for the smallest two  $1/N_q$  values. Therefore, we report two values for SiC-4H in Table III; the difference in  $\Delta E_{av}^{ep}(0)$  a) between the smallest values of  $1/N_q$  for SiC-3C and SiC-4H and b) at approximately the same  $1/N_q \approx 0.039$ . The actual stability value for SiC-4H is likely to be between these values.

Table III shows the importance of EPI corrections. SiC-4H is the stable polytype with much greater relative stability ( $\geq 20$  meV/f.u.), irrespective of the DFT-D approximation, compared to the marginal stability ( $\approx 2$  meV/f.u.) under DFT and DFT+vdW conditions. For SiC-2H, the relative stability depends on the DFT-D approximation used, though it is more stable in the widely used D3(BJ) approximation [17, 54]. However, the stability is  $< 10$  meV/f.u., indicating that it is within the range of dispersion approximation errors [17].

TABLE III. Relative stability (meV/f.u.) of SiC polytypes. In column-3, the second value corresponds to  $1/N_q \approx 0.039$ . The D2 values are estimated from DFT and D3(BJ) values as its lattice parameters are in-between their lattice parameters.

Polytype $\rightarrow$	SiC-3C	SiC-4H	SiC-2H
DFT + EPI (100meV)	0	-30.8/-25.5	-5.7
DFT-D2 + EPI (100 meV)	0	-25.6/-19.9	+2.8
DFT-D3(BJ) + EPI (100meV)	0	-30.0/-24.0	-5.6
DFT-D3(BJ) + EPI (50meV)	0	-32.9/-27.6	-8.5

The similar trends for  $i\delta = 50$  meV suggests that SiC-4H will likely be the stable polytype when  $i\delta$  is decreased further for full convergence [34].

With our results, we can assess the importance of the three correction terms to the DFT relative stability order of SiC polytypes. The ZPVE is relatively insensitive to crystal structure [13] which is also reflected in the similar Debye temperatures of SiC polytypes [55, 56]. The D3(BJ) correction is also relatively insensitive to crystal structure. Both these terms contribute  $\sim 1$ -2 meV/f.u.

each to the energy differences between SiC polytypes. In contrast, EPI correction contributes  $\geq 22$  meV/f.u. to the energy differences (Figure 2) indicating much greater sensitivity to crystal structure. Hence, the EPI term is the most important of the three correction terms to affect the relative stability of SiC polytypes.

After including ZPVE, vdW and EPI corrections to DFT, the relative stability order is SiC-4H, SiC-2H and SiC-3C; that is, SiC-3C is clearly metastable. To resolve the discrepancy between *ab initio* and experimental results for SiC polytypes further studies are required.

We can also calculate the EPI corrections at finite temperatures. Figure 3 shows that at higher temperatures,  $\Delta\epsilon_{vbm}(T)$  varies linearly with temperature, as predicted for all eigenstates [26]. The slope is  $\lesssim 0.2$  meV/K similar to predicted values [22, 26]. In particular, the experimentally obtained slope for SiC-6H is 0.24 meV/K [57]. Our values are acceptable as the calculated values are known to be smaller than the experimental values of the slope (for bandgaps) in other materials [34].

It follows that the weighted sum,  $\Delta E_{av}^{ep}(T)$ , will also vary linearly with temperature and is seen in Figure 3. We note that  $\Delta\epsilon_{nk}(T)$  has both positive and negative values. For this reason, despite  $8 e^-$ /f.u., the temperature variation of weighted sum,  $\Delta E_{av}^{ep}(T)$ , is only slightly larger, and not  $\approx 8$  times larger, than that for  $\Delta\epsilon_{vbm}(T)$ .

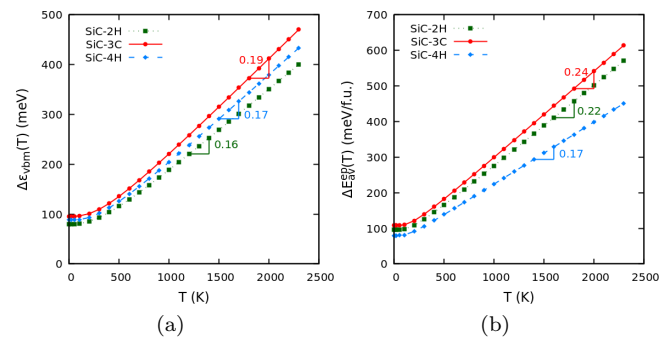


FIG. 3. Finite temperature EPI corrections to (a) VBM and (b) total energy of SiC for DFT-D3(BJ) lattice parameters.

The thermodynamic properties are obtained from QHA where the Helmholtz free energy is given by [58, 59]

$$F(V, T) = E_0(V) + F_{vib}(V, T) + F_{elec}(V, T) \quad (4)$$

where  $E_0(V)$  is the DFT total energy,  $F_{vib}(V, T)$  is the vibrational free energy contribution and  $F_{elec}(V, T)$  is the electronic contribution. Because the EPI contribution (Eq. 3) is now represented separately, it can be added in Eq. (4) above.

Even after the EPI corrections are included, because the band gaps are of order eV, the electronic specific heat is  $\approx 0$ , consistent with experiments [60]. Theoretically, the EPI contribution to specific heat is negligible because the product  $[f(\epsilon)(1 - f(\epsilon))] \approx 0$  [24]. In QHA, from Eq.

(4), the EPI contribution to specific heat is obtained as  $\Delta C_v^{ep}/T = -F''_{epi}(T) = -\Delta E_{av}^{ep}(T)$ . From Figure 3, at low temperatures,  $\Delta E_{av}^{ep}(T)$  is constant and at high temperatures its first derivative is constant. Therefore,  $\Delta C_v^{ep}(T) \approx 0$  at low and high temperatures, consistent with theory and experiments. In a small intermediate temperature range, an error is given that is unavoidable as  $\Delta E_{av}^{ep}(V, T)$  changes from constant value to linear dependence on temperature, leading to finite second derivative. In Figure 3, in the intermediate temperature range (100 K - 500 K), we estimate  $-\Delta C_v^{ep}$  at 200 K to be  $\approx 0.13, 0.12$  and  $0.09$  meV/K.f.u which drops rapidly at 300 K to  $0.07, 0.06$  and  $0.03$  meV/K.f.u. for SiC-3C, SiC-2H and SiC-4H respectively. The magnitudes are comparable to the vibrational specific heat at 200 K and are much less at 300 K [61]. Thus, because the errors are limited to a small temperature range, the role of EPI can be incorporated in QHA through  $\Delta E_{av}^{ep}(V, T)$ .

The differences in the thermodynamic properties (lattice parameters (and those dependent on them), thermal expansion, etc.) evaluated from Eq. (4) with and without  $\Delta E_{av}^{ep}(V, T)$  are the EPI contribution to the properties. The former is more appropriate for comparison with experimental values which include EPI contributions.

Our results have wide applicability. A significant EPI results in ZPR of VBM and other eigenstates in hundreds of meV in several materials [30–42]. It also leads to strong crystal structure dependence of the ZPR(VBM) with its differences in tens of meV in AlN, BN and GaN polytypes [34, 40, 42]. Because the ZPR(VBM) contributes to  $\Delta E_{av}^{ep}(0)$ , it follows that differences in  $\Delta E_{av}^{ep}(0)$  between polymorphs of order of tens of meV/f.u. is a distinct possibility that must be evaluated. Our results for C and SiC polytypes support this suggestion.

In conclusion, we introduce a new correction term due to electron-phonon interactions to the DFT total energy. The EPI corrections alter the energy differences between polytypes in C, Si and SiC; especially in C and SiC where the EPI strength is significant. It clearly establishes that in *ab initio* studies SiC-3C is metastable and SiC-4H is the stable polytype. Compared to the ZPVE and vdW correction, the EPI correction term is more important in determining the relative stability order of SiC polytypes due to its greater sensitivity to crystal structure. For these studies, we extend Allen's formalism and this enables, for the first time, inclusion of EPI corrections as separate terms in the free energy in QHA. This opens the way to study their role on all thermodynamic properties.

---

\* prasanna@iitb.ac.in

[1] M. Takagi, T. Taketsugu, H. Kino, Y. Tateyama, K. Terakura, and S. Maeda, *Physical Review B* **95**, 184110 (2017).  
 [2] A. Mujica, C. J. Pickard, and R. J. Needs, *Physical Review B* **91**, 214104 (2015).

[3] C. He, X. Shi, S. J. Clark, J. Li, C. J. Pickard, T. Ouyang, C. Zhang, C. Tang, and J. Zhong, *Physical Review Letters* **121**, 175701 (2018).  
 [4] V. E. Dmitrienko and V. A. Chizhikov, *Physical Review B* **101**, 245203 (2020).  
 [5] B. Haberl, T. A. Strobel, and J. E. Bradby, *Applied Physics Reviews* **3**, 040808 (2016).  
 [6] D. M. Proserpio, Samara carbon allotrope database, <http://sacada.sctms.ru> (accessed July 15, 2021).  
 [7] I.-H. Lee, J. Lee, Y. J. Oh, S. Kim, and K.-J. Chang, *Physical Review B* **90**, 115209 (2014).  
 [8] F. Riley, *Structural Ceramics* (Cambridge, UK: Cambridge University Press, 2009).  
 [9] T. Kimoto, *Japanese Journal of Applied Physics* **54**, 040103 (2015).  
 [10] C. H. Park, B.-H. Cheong, K.-H. Lee, and K.-J. Chang, *Physical Review B* **49**, 4485 (1994).  
 [11] P. Käckell, B. Wenzien, and F. Bechstedt, *Physical Review B* **50**, 10761 (1994).  
 [12] S. Kawanishi and T. Mizoguchi, *Journal of Applied Physics* **119**, 175101 (2016).  
 [13] E. Scalise, A. Marzeggalli, F. Montalenti, and L. Miglio, *Physical Review Applied* **12**, 021002 (2019).  
 [14] V. Heine, C. Cheng, and R. J. Needs, *Journal of the American Ceramic Society* **74**, 2630 (1991).  
 [15] M. J. Rutter and V. Heine, *Journal of Physics: Condensed Matter* **9**, 8213 (1997).  
 [16] T. Gruber and A. Grüneis, *Physical Review B* **98**, 134108 (2018).  
 [17] C. Cazorla and T. Gould, *Science Advances* **5**, eaau5832 (2019).  
 [18] M. J. van Setten, M. A. Uijtewaal, G. A. de Wijs, and R. A. de Groot, *Journal of the American Chemical Society* **129**, 2458 (2007).  
 [19] S. S. Bhat, K. Gupta, S. Bhattacharjee, and S.-C. Lee, *Journal of Physics: Condensed Matter* **30**, 215401 (2018).  
 [20] F. Giustino, *Reviews of Modern Physics* **89**, 015003 (2017).  
 [21] S. Poncé, G. Antonius, Y. Gillet, P. Boulanger, J. L. Janssen, A. Marini, M. Côté, and X. Gonze, *Physical Review B* **90**, 214304 (2014).  
 [22] P. B. Allen and V. Heine, *Journal of Physics C: Solid State Physics* **9**, 2305 (1976).  
 [23] P. B. Allen, *Physical Review B* **18**, 5217 (1978).  
 [24] P. B. Allen and J. C. K. Hui, *Zeitschrift für Physik B Condensed Matter* **37**, 33 (1980).  
 [25] P. B. Allen and M. Cardona, *Physical Review B* **27**, 4760 (1983).  
 [26] P. B. Allen, *Philosophical Magazine B* **70**, 527 (1994).  
 [27] H. Y. Fan, *Physical Review* **82**, 900 (1951).  
 [28] A. B. Migdal, *Soviet Physics-JETP* **7**, 996 (1958).  
 [29] E. Antončík, *Czechoslovak Journal of Physics* **5**, 449 (1955).  
 [30] A. Marini, *Physical Review Letters* **101**, 106405 (2008).  
 [31] F. Giustino, S. G. Louie, and M. L. Cohen, *Physical Review Letters* **105**, 265501 (2010).  
 [32] G. Antonius, S. Poncé, P. Boulanger, M. Côté, and X. Gonze, *Physical Review Letters* **112**, 215501 (2014).  
 [33] S. Poncé, G. Antonius, P. Boulanger, E. Cannuccia, A. Marini, M. Côté, and X. Gonze, *Computational Materials Science* **83**, 341 (2014).  
 [34] S. Poncé, Y. Gillet, J. Laflamme Janssen, A. Marini, M. Verstraete, and X. Gonze, *The Journal of Chemical*

- Physics **143**, 102813 (2015).
- [35] G. Antonius, S. Poncé, E. Lantagne-Hurtubise, G. Auclair, X. Gonze, and M. Côté, *Physical Review B* **92**, 085137 (2015).
- [36] C. E. Patrick and F. Giustino, *Journal of Physics: Condensed Matter* **26**, 365503 (2014).
- [37] M. Zacharias and F. Giustino, *Physical Review B* **94**, 075125 (2016).
- [38] M. Friedrich, A. Riefer, S. Sanna, W. Schmidt, and A. Schindlmayr, *Journal of Physics: Condensed Matter* **27**, 385402 (2015).
- [39] J. P. Nery, P. B. Allen, G. Antonius, L. Reining, A. Miglio, and X. Gonze, *Phys. Rev. B* **97**, 115145 (2018).
- [40] R. Tutchton, C. Marchbanks, and Z. Wu, *Physical Review B* **97**, 205104 (2018).
- [41] J. D. Querales-Flores, J. Cao, S. Fahy, and I. Savić, *Physical Review Materials* **3**, 055405 (2019).
- [42] A. Miglio, V. Brousseau-Couture, E. Godbout, G. Antonius, Y.-H. Chan, S. G. Louie, M. Côté, M. Giantomassi, and X. Gonze, *Npj Computational Materials* **6**, 1 (2020).
- [43] P. B. Allen, *Modern Physics Letters B* **34**, 2050025 (2020).
- [44] C. Asker, A. B. Belonoshko, A. S. Mikhaylushkin, and I. A. Abrikosov, *Physical Review B* **77**, 220102 (2008).
- [45] F. Yang, J. Muñoz, O. Hellman, L. Mauger, M. Lucas, S. Tracy, M. Stone, D. Abernathy, Y. Xiao, and B. Fultz, *Physical Review Letters* **117**, 076402 (2016).
- [46] X. Gonze, B. Amadon, P.-M. Anglade, J.-M. Beuken, F. Bottin, P. Boulanger, F. Bruneval, D. Caliste, R. Caracas, M. Côté, *et al.*, *Computer Physics Communications* **180**, 2582 (2009).
- [47] X. Gonze, F. Jollet, F. A. Araujo, D. Adams, B. Amadon, T. Applencourt, C. Audouze, J.-M. Beuken, J. Bieder, A. Bokhanchuk, *et al.*, *Computer Physics Communications* **205**, 106 (2016).
- [48] Abinit, tutorial tdepes, temperature-dependence of the electronic structure., <https://docs.abinit.org/tutorial/tdepes/>, accessed: 2020-03-15.
- [49] S. Grimme, *Journal of Computational Chemistry* **27**, 1787 (2006).
- [50] S. Grimme, S. Ehrlich, and L. Goerigk, *Journal of Computational Chemistry* **32**, 1456 (2011).
- [51] B. Van Troeye, M. Torrent, and X. Gonze, *Physical Review B* **93**, 144304 (2016).
- [52] C. Raffy, J. Furthmüller, and F. Bechstedt, *Physical Review B* **66**, 075201 (2002).
- [53] Q. Fan, C. Chai, Q. Wei, K. Wong, Y. Liu, and Y. Yang, *Journal of Materials Science* **53**, 2785 (2018).
- [54] M. Stöhr, T. Van Voorhis, and A. Tkatchenko, *Chem. Soc. Rev.* **48**, 4118 (2019).
- [55] W.-W. Xu, F. Xia, L. Chen, M. Wu, T. Gang, and Y. Huang, *Journal of Alloys and Compounds* **768**, 722 (2018).
- [56] V. L. Moruzzi, J. F. Janak, and K. Schwarz, *Physical Review B* **37**, 790 (1988).
- [57] P. S. Miedema, M. Beye, R. Könnecke, G. Schiwietz, and A. Föhlisch, *Journal of Electron Spectroscopy and Related Phenomena* **197**, 37 (2014).
- [58] A. Togo and I. Tanaka, *Scripta Materialia* **108**, 1 (2015).
- [59] P. Nath, J. J. Plata, D. Usanmaz, R. A. R. Al Orabi, M. Fornari, M. B. Nardelli, C. Toher, and S. Curtarolo, *Computational Materials Science* **125**, 82 (2016).
- [60] W. A. Harrison, *Solid state theory* (Dover, 1980).
- [61] A. Zywietz, K. Karch, and F. Bechstedt, *Physical Review B* **54**, 1791 (1996).

## Supplementary Information for

### Electron-phonon interaction correction to the total energy of group IV semiconductor polytypes

R. Arjun Varma,<sup>1</sup> Shilpa Paul,<sup>1</sup> Anup Itale,<sup>1</sup> Pranav Pable,<sup>1</sup> Radhika Tibrewala,<sup>1</sup> Samruddhi Dodal,<sup>1</sup> Harshal Yerunkar,<sup>1</sup> Saurav Bhowmick,<sup>2</sup> Vaishali Shah,<sup>3</sup> M. P. Gururajan,<sup>1</sup> and T. R. S. Prasanna<sup>1,\*</sup>

<sup>1</sup>*Department of Metallurgical Engineering and Materials Science,  
Indian Institute of Technology Bombay, Mumbai 400076, India*

<sup>2</sup>*Department of Mathematics, Indian Institute of Technology Bombay, Mumbai 400076, India*

<sup>3</sup>*Department of Scientific Computing, Modeling and Simulation,  
Savitribai Phule Pune University, Pune 411007, India*

(Dated: April 19, 2022)

In the Supplementary Information, we present: (i) Extension of Allen's formalism to include EPI corrections (Section I), (ii) Supporting evidence, (Section II) (iii) Proof of linearity of the EPI correction to the total energy (Section III) and (iv) Results for the GGA.fhi (PBE) and the pspnc (LDA) pseudopotentials for Si, C (Section IV) and SiC polytypes (Section V) respectively.

#### I. EXTENSION OF ALLEN'S FORMALISM TO INCLUDE EPI CORRECTIONS

Allen [S1] has discussed incorporating EPI corrections in QHA. In this paper, in Sec-VI titled "Corrections to the QH theory from QP renormalization" Allen states "QH theory puts the first two terms of the energies in Eqs. 1 and 2 into the free energy Eqs. 11 and 12. To get the renormalization corrections  $\Delta F_{renorm}$  from  $\Delta\epsilon_K^{QP}$  and  $\Delta\omega_K^{QP}(V, T)$ , use the entropy formulas 23 and 24 with the full QP energies in Eqs. 1 and 2." The reason for two different methods to calculate the free energy is described by Allen as "It is unfortunately incorrect to insert the full renormalized energies into the noninteracting free energy  $F_{QH}$ ".

Because Eq.1 and Eq.23 pertain to electrons and Eq.2 and Eq.24 pertain to phonons, we reproduce the former equations that are relevant to the present study.

Eq.1 of Allen [S1] is

$$\epsilon_K^{QP}(V, T) = \epsilon_K(V_0) + \Delta\epsilon_K^{QH} + \Delta\epsilon_K^{QP}(V, T) \quad (S1)$$

The first term is the eigenenergy for static lattice parameters. The second term is the change in eigenenergy when vibrational free energy is included to determine the equilibrium lattice parameters. The third term is the contribution of interactions (e.g. EPI).

Eq.23 of Allen [S1] is

$$S_{el} = -k_B \sum_K [f_K \ln f_K + (1 - f_K) \ln(1 - f_K)] \quad (S2)$$

At the outset, it is clear from Allen's statements above that the change in the method to calculate the free energy, from (i) Eq.11 to (ii) Eq.1 plus Eq.23, is due to the inclusion of the third term, which corresponds to quasiparticle interactions.

The method for non-interacting particles is to be used when only the first two terms in Eq.1 are considered. However, including the third term in Eq.1 of Allen means that quasiparticles interact and the first method can no longer be used. Hence, the other method to calculate free energy from Eq.1 plus Eq.23 must be used. The

---

\* prasanna@iitb.ac.in

difference in free energies calculated from these two methods,  $\Delta F_{renorm}$ , is the EPI contribution to the free energy. This is Allen's formalism to include the contributions from quasiparticle interactions in QHA.

Allen states "Finally, consider electron-phonon interactions" and represents the EPI correction to the eigenenergy as  $\Delta_{ep}\epsilon_K^{QP}$ . From the structure of the symbol, it is clear that it is in the category of the third term in Eq.1 of Allen. Hence, we have to calculate the free energies from both methods described above and their difference is the EPI correction to the free energy,  $\Delta F_{epi}(V, T)$ .

We first calculate the free energy from the first method, Eq.11, whose first line is given as

$$F_{el}^{QH}(V, T) = k_B T \sum_K \ln(1 - f_{K0}(V, T)) \quad (S3)$$

where  $f_K$  is the Fermi-Dirac distribution given by

$$f_K = \frac{1}{\exp(\frac{(\epsilon_K(V) - \mu(V))}{k_B T}) + 1} \quad (S4)$$

It is clear from Eq.11 of Allen that  $\epsilon_K(V)$  is the energy to be used above and from Eq.3 of Allen it is seen to be the sum of the first two terms in Eq.1 of Allen.

Substituting Eq. S4 in Eq. S3 leads to

$$F_{el}^{QH}(V, T) = k_B T \sum_K \ln\left(\frac{\exp(\frac{(\epsilon_K(V) - \mu(V))}{k_B T})}{\exp(\frac{(\epsilon_K(V) - \mu(V))}{k_B T}) + 1}\right) \quad (S5)$$

In semiconductors and insulators, the occupied energy levels are well below the Fermi level, due to which the exponential term is negligible and the free energy becomes

$$F_{el}^{QH}(V, T) = \sum_K (\epsilon_K(V) - \mu(V)) \rightarrow E_{el}(V) \quad (S6)$$

Eq. S6 is identical to the first term in line-2 of Eq.11 of Allen.

We next calculate the free energy by the second method, from Eq.1 plus Eq.23 of Allen. For semiconductors and insulators, in Eq.23 of Allen (Eq. S2),  $f_K \approx 1$  and the entropy contribution is  $\approx 0$ . Thus, the free energy contribution reduces to the contribution from the energy term. This is given by the summation over occupied states of all the three terms in Eq.1 of Allen (Eq. S1) above.

$$F_{el}^{QH}(V, T) = \sum_K (\epsilon_K(V_0) + \Delta\epsilon_K^{QH} + \Delta_{ep}\epsilon_K^{QP}(V, T)) \quad (S7)$$

From Eq.3 of Allen, the sum of the first two energy terms is  $\epsilon_K(V)$  and the free energy can be written as

$$F_{el}^{QH}(V, T) = \sum_K \epsilon_K(V) + \sum_K \Delta_{ep}\epsilon_K^{QP}(V, T) \rightarrow E_{el}(V) + \sum_K \Delta_{ep}\epsilon_K^{QP}(V, T) \quad (S8)$$

Regarding the arrow in Eq. S6, Allen states "In the third and fourth lines of Eq. 11, the zero-point electronic contribution ( $\sum_K (\epsilon_K(V) - \mu(V))$ ) has been replaced by a more accurate electronic T = 0 frozen lattice energy,  $E_{el}(V)$ . This is computed, for example, by DFT." In such a case, a similar change must also be made for the equivalent term,  $\sum_K \epsilon_K(V)$ , in Eq. S8.

The difference in the free energies from the two methods (Eq. S8 - Eq. S6) is the renormalization of the free energy,  $\Delta F_{renorm}$ , due to EPI corrections. In our paper,  $\Delta F_{renorm}$  is referred to as  $\Delta F_{epi}(V, T)$  and is given by

$$\Delta F_{epi}(V, T) = \sum_K \Delta_{ep}\epsilon_K^{QP}(V, T) = \Delta E_{av}^{ep}(V, T) \quad (S9)$$

Thus, for semiconductors and insulators, the EPI contribution to the free energy is due to the EPI contribution to the band-structure energy. This is represented as Eq.3 in the main paper.

Because the entropy contribution is zero for semiconductors and insulators, it follows that the EPI correction to the total energy is also equal to the EPI correction to the band-structure energy. This is represented as Eq.2 in the main paper.

The above formalism applied to metals results in additional terms in the free energy that are not present in semiconductors and insulators. In the first method to calculate free energy, the second term in Eq.11 of Allen [S1] is non-zero. In the second method, the entropy contribution is non-zero.

For the energy term, a minor contribution comes from the electron occupancies that are temperature dependent through the Fermi-Dirac distribution. However, the main contribution is from the inclusion of the third term due to EPI,  $\Delta_{ep}\epsilon_K^{QP}(V, T)$ . For total energy contribution, this term must be summed over occupied states. Thus, the EPI contribution to the band-structure energy is the main term in the EPI contribution to the total energy. That is, Eq.2 of the main paper is the main energy correction term in metals as well.

Thus, Eq.2 of the main paper is a result of general validity and is applicable for all classes of materials - metals, semiconductors and insulators. Further, because it does not depend on the method of calculation of EPI, it is applicable to results from all EPI calculation methods, AIMD, Allen-Heine theory and other methods.

## II. SUPPORTING EVIDENCE

In some metallic systems, Mo [S2], Zr [S3], FeTi [S4], *ab initio* molecular dynamics (AIMD) studies show that the electronic density of states (EDOS) is temperature dependent and at high temperatures the sharp features of the EDOS are smoothed. This has been attributed to adiabatic EPI [S4]. It is clear that in such systems, EPI causes the EDOS and hence, the band-structure energy to be temperature dependent. From Eq.2 of the main paper, it follows that this temperature dependent band-structure energy is equal to and hence, should be the main cause for the temperature dependence of the total energy.

Asker et al. [S2] have used AIMD to determine the temperature dependent energy differences between bcc and fcc Mo. Static lattice calculations show that the energy difference between bcc and fcc Mo structures is 400 meV/atom at 0 K. At high temperatures, using AIMD, they obtain a configuration energy difference of 190 meV/atom. They attribute this difference to the differences in the electronic density of states (EDOS) for static lattice and vibrating lattice conditions.

They state [S2] “The results are shown in Fig.3. It is clear that the average DOS from the AIMD simulations is different from the DOS for the ideal lattice structures. One can clearly see that the thermal motion smears out most of the peculiarities of the DOS. Because of this the large difference between the DOS calculated for the ideal bcc and fcc crystal lattices becomes much less pronounced, especially around the Fermi level. As a matter of fact, this indicates that the configurational energies of the two phases must be much closer to each other, as compared to the T=0 K values.”

They also state [S2] “thermal motion at high temperature destroys the canonical shape of the DOS, as we explained above, and makes the electronic structure of the two phases much more similar to each other, leading to a strong temperature dependence of the lattice stability.”

It is clear that in the above study, adiabatic EPI causes the EDOS (and hence, the band structure energy) to be temperature dependent and this in turn causes the total energy to be temperature dependent. This is entirely consistent with the main result for the EPI correction to the total energy mentioned above. Thus, the study of Asker et al. provides supporting evidence for the extension of Allen’s formalism for the EPI correction to the total energy (Eq.2 of main paper). Indeed, Eq. 2 is the theoretical basis for the computational results of Asker et al. [S2].

### III. PROOF THAT $\Delta E_{av}^{ep}(T)$ VARIES LINEARLY WITH $1/N_q$

For brevity, we represent  $\Delta\epsilon_{n\mathbf{k}}(T)$  as  $\Delta\epsilon_{n\mathbf{k}}$ . Given that  $\Delta\epsilon_{n\mathbf{k}}$  is linear in  $x$  ( $= 1/N_q$ ) for all  $n, \mathbf{k}$ , there are constants,  $a_{n\mathbf{k}}$  and  $b_{n\mathbf{k}}$  such that:

$$\Delta\epsilon_{n\mathbf{k}}(x) = a_{n\mathbf{k}}x + b_{n\mathbf{k}} \quad (\text{S10})$$

The converged eigenvalue,  $\Delta\epsilon_{n\mathbf{k}}^c$ , is given by:

$$\Delta\epsilon_{n\mathbf{k}}^c = \lim_{x \rightarrow 0^+} \Delta\epsilon_{n\mathbf{k}}(x) = b_{n\mathbf{k}} \quad (\text{S11})$$

Substituting Eq. (S10) in Eq. (S11), we get:

$$\Delta E_{av}^{ep}(x) = 2x \sum_{n\mathbf{k}}^{occ,IBZ} w_{\mathbf{k}} a_{n\mathbf{k}} + 2 \sum_{n\mathbf{k}}^{occ,IBZ} w_{\mathbf{k}} b_{n\mathbf{k}} \quad (\text{S12})$$

The converged value of the EPI correction to the total energy,  $\Delta E_{av}^{ep,c}$ , is given by:

$$\Delta E_{av}^{ep,c} = \sum_{n\mathbf{k}}^{occ,IBZ} w_{\mathbf{k}} \Delta\epsilon_{n\mathbf{k}}^c = 2 \sum_{n\mathbf{k}}^{occ,IBZ} w_{\mathbf{k}} b_{n\mathbf{k}} \quad (\text{S13})$$

Therefore,

$$\Delta E_{av}^{ep,c} = \lim_{x \rightarrow 0^+} E_{av}^{ep}(x) \quad (\text{S14})$$

It follows from Eq. (S12) and Eq. (S14) that  $\Delta E_{av}^{ep}(T)$  varies linearly with  $1/N_q$  and the converged value can be obtained by linear extrapolation.

### IV. SI AND C POLYMORPHS

Figure S1 shows the convergence behavior of the EPI correction to the total energy with q-point grid density, using the GGA.fhi pseudopotential.

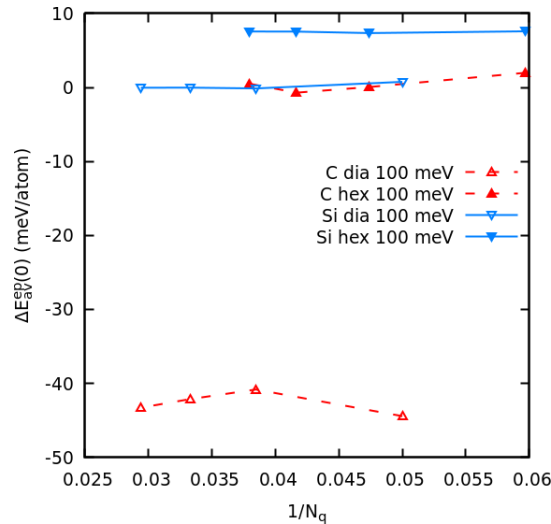


FIG. S1. Convergence of electron-phonon interaction correction to the total energy with q-point grid density for smearing parameter value of 100 meV for carbon and silicon polytypes for GGA.fhi pseudopotential.

Table S1 gives the lattice parameters, band gaps and the relative energy stability with and without EPI corrections for the C and Si polymorphs. The increase in relative stability of C-dia and Si-dia is clearly seen when the EPI corrections to the total energies are included.

Figure S2 shows the convergence behavior of the EPI correction to the total energy with q-point grid density using the pspnc pseudopotential.

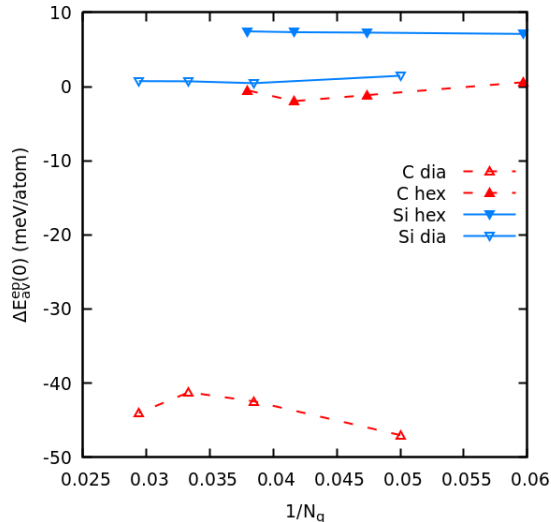


FIG. S2. Convergence of electron-phonon interaction correction to the total energy with q-point grid density for smearing parameter value of 100 meV for carbon and silicon polytypes for pspnc (LDA) pseudopotential.

Table S2 gives the lattice parameters, band gaps and the relative energy stability with and without EPI corrections for the C and Si polymorphs. The increase in relative stability of C-dia and Si-dia is clearly seen when the EPI corrections to the total energies are included.

TABLE S2. The lattice parameters, band gaps and the energy differences for carbon and silicon polytypes (DFT and DFT+EPI, in meV/f.u.) for pspnc pseudopotential

Material	a,c (Bohr)	Band gaps (Indirect/ Direct) (eV)	$\Delta E$ (DFT)	$\Delta E$ (DFT+EPI)
C-dia	6.69	4.22, 5.63	0	0
C-hex	4.706, 7.838	3.12, 4.99	24.8	68.5
Si-dia	10.20	0.43, 2.52	0	0
Si-hex	7.180, 11.875	0.26, 0.95	8.4	15.1

The above results are similar to those for ONCV pseudopotential in the main paper.

TABLE S1. The lattice parameters, band gaps and the energy differences for carbon and silicon polytypes (DFT and DFT+EPI, in meV/f.u.) for GGA.fhi pseudopotential

Material	a,c (Bohr)	Band gaps (Indirect/ Direct) (eV)	$\Delta E$ (DFT)	$\Delta E$ (DFT+EPI)
C-dia	6.73	4.21, 5.62	0	0
C-hex	4.732, 7.876	3.38, 5.0	24.9	68.7
Si-dia	10.33	0.614, 2.56	0	0
Si-hex	7.27, 12.017	0.45, 0.98	9.8	17.4

TABLE S3. The lattice parameters and the energy stability of SiC polytypes relative to SiC-3C for DFT, DFT-D2 and DFT-D3(BJ) conditions for GGA.fhi pseudopotential.

Polytype	a,c (Bohr)	$\Delta E$ (meV/SiC)
<b>3C-SiC</b>		
DFT	8.26	0
DFT-D2	8.21	0
DFT-D3(BJ)	8.20	0
<b>6H-SiC</b>		
DFT	5.836, 28.637	-2.16
DFT-D2	5.802, 28.495	0.91
DFT-D3(BJ)	5.789, 28.409	-1.98
<b>4H-SiC</b>		
DFT	5.834, 19.099	-2.11
DFT-D2	5.799, 19.014	2.54
DFT-D3(BJ)	5.788, 18.498	-1.84
<b>2H-SiC</b>		
DFT	5.831, 9.568	4.98
DFT-D2	5.795, 9.537	14.5
DFT-D3(BJ)	5.784, 9.491	6.02

## V. SiC POLYTYPES

We first present results for SiC polytypes obtained using GGA.fhi pseudopotential.

Table S3 shows the lattice parameters and the energy stabilities relative to the SiC-3C polytype for DFT condition and also when dispersion approximations are included. We see that SiC-4H is more stable than SiC-3C for DFT conditions. When vdW-D2 approximation is included, SiC-3C is the stable structure, similar to literature results. However, when vdW-D3(BJ) approximation is used, SiC-4H is more stable. This is similar to the results for the ONCV pseudopotential reported in the main paper.

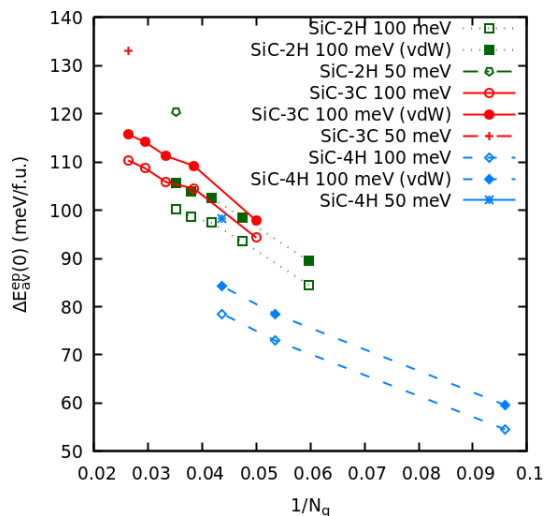


FIG. S3. Convergence of EPI correction to the total energy with q-point grid density for different smearing parameters for SiC polytypes for DFT and DFT-D3(BJ) lattice parameters for GGA.fhi pseudopotential.

Figure S3 shows the convergence behaviour of the EPI correction to the total energy with q-point grid density for SiC polytypes for different smearing parameters. For 100 meV smearing parameter, the  $\Delta E_{av}^{ep}(0)$  was calculated only upto  $\frac{1}{N_q} \approx 0.043$  due to computational limitations. For 50 meV smearing parameter, only the results for the highest

q-point grid density was calculated (due to computational limitations.)

TABLE S4. Relative stability (in meV/f.u.) of SiC polytypes using GGA.fhi pseudopotential in non-adiabatic condition-100meV smearing parameter. vdW represents results from DFT+D3(BJ) calculations .

Polytype→ Stability ↓	SiC-3C	SiC-4H	SiC-2H
DFT	0	-2.1	5.0
DFT + vdW	0	-1.8	6.0
DFT + EPI (100meV)	0	-33.9/-28.1	-5.1
DFT + vdW + EPI (100meV)	0	-33.4/-26.8	-4.1
DFT + vdW + EPI (50meV)	0	-36.6	-6.7

Table S4 shows the final stability of SiC-polytypes obtained by combining the EPI corrections in Figure S3 with the relative stability data in Table S3. For SiC-3C and SiC-2H we consider the last value to be the converged value. However, for SiC-4H, the last calculatee value ( $\frac{1}{N_q} \approx 0.043$ ) is not the converged value as it varies by  $\lesssim 6$  meV/f.u. compared to the previous value. Therefore, for SiC-4H, we report two values in Table S4; the first is the difference between the last values for SiC-3C and SiC-4H and the second is the difference at  $\frac{1}{N_q} \approx 0.043$  for SiC-4H and the nearest value for SiC-3C,  $\frac{1}{N_q} \approx 0.039$ . The actual stability value of for SiC-4H is likely to be between these two values.

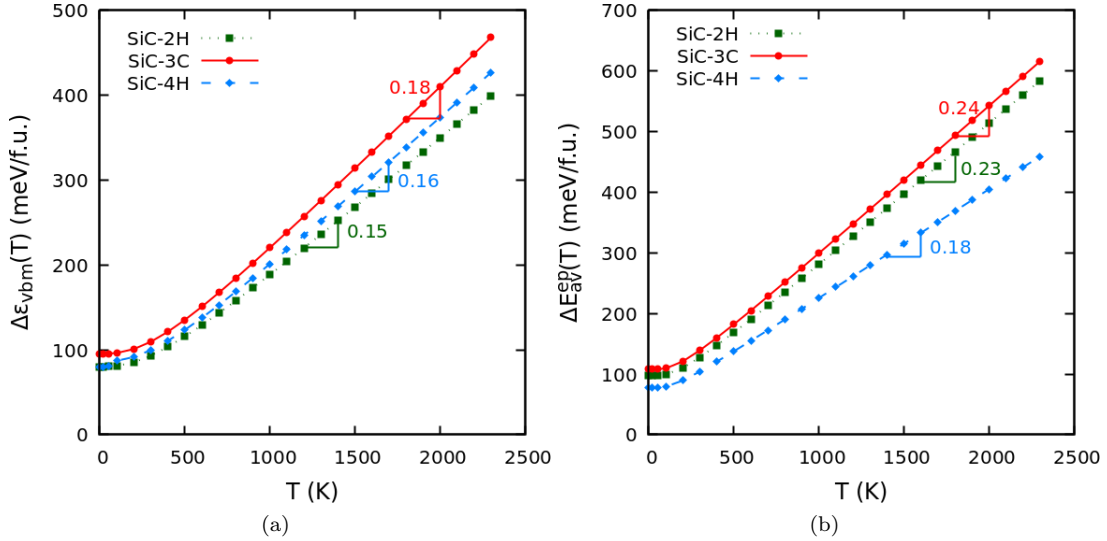


FIG. S4. Finite temperature EPI corrections to (a) VBM and (b) total energy of SiC for DFT-D3(BJ) lattice parameters for GGA.fhi pseudopotential.

Figure S4 shows temperature dependence of the EPI correction to VBM and the total energy for SiC polytypes for GGA.fhi pseudopotential.

The results using GGA.fhi pseudopotential are similar to those from ONCV-PBE pseudopotential presented in the main paper.

Table S5 shows the lattice parameters and the energy stabilities relative to the SiC-3C polytype using the pspnc pseudopotential. The vdW corrections were not performed because ABINIT package does not support DFT-D2 and DFT-D3(BJ) corrections for LDA pseudopotentials.

TABLE S5. The lattice parameters and the energy stability (DFT) in meV/f.u. of SiC polytypes relative to SiC-3C for DFT lattice parameters for pspnc pseudopotential.

Polytype	a,c (Bohr)	$\Delta E$ (DFT)
<b>3C-SiC</b>		
DFT	8.18	0
<b>6H-SiC</b>		
DFT	5.784, 28.383	-2.16
<b>4H-SiC</b>		
DFT	5.782, 18.931	-3.17
<b>2H-SiC</b>		
DFT	5.778, 9.485	4.33

Figure S5 shows the convergence behaviour of the EPI correction to the total energy with q-point grid density for SiC polytypes for different smearing parameters. For 100 meV smearing parameter, the  $\Delta E_{av}^{ep}(0)$  was calculated only upto  $\frac{1}{N_q} \approx 0.043$  due to computational limitations. For 50 meV smearing parameter, only the results for the highest q-point grid density was calculated (due to computational limitations.)

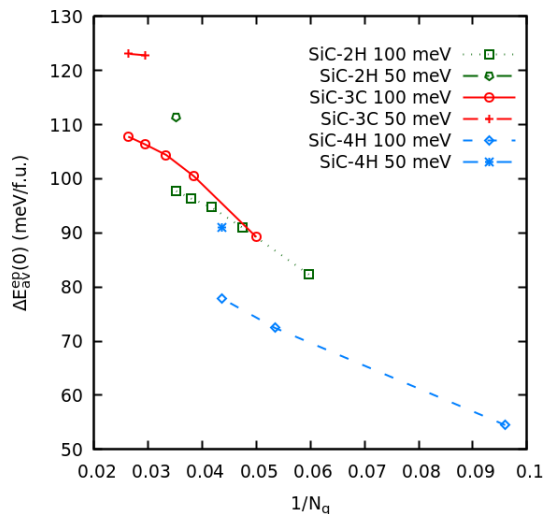


FIG. S5. Convergence of electron-phonon interaction correction to the total energy with q-point grid density for different values of the smearing parameter for SiC polytypes for pspnc (LDA) pseudopotential.

TABLE S6. Relative stability (in meV/f.u.) of SiC polytypes using pspnc pseudopotential in non-adiabatic condition-100 meV and 50 meV smearing parameters.

Polytype → Stability ↓	SiC-3C	SiC-4H	SiC-2H
DFT	0	-3.2	4.3
DFT + EPI (100 meV)	0	-33.1/-25.8	-5.7
DFT + EPI (50 meV)	0	-35.2	-7.3

Table S6 shows the final stability of SiC-polytypes obtained by combining the EPI corrections in Figure S4 with the relative stability data in Table S5. For SiC-3C and SiC-2H we consider the last value to be the converged value. However, for SiC-4H, the last calculatee value ( $\frac{1}{N_q} \approx 0.043$ ) is not the converged value as it varies by  $\lesssim 6$  meV/f.u. compared to the previous value. Therefore, for SiC-4H, we report two values in Table S4; the first is the difference between the last values for SiC-3C and SiC-4H and the second is the difference at  $\frac{1}{N_q} \approx 0.043$  for SiC-4H and the nearest value for SiC-3C,  $\frac{1}{N_q} \approx 0.039$ . The actual stability value of for SiC-4H is likely to be between these two values.

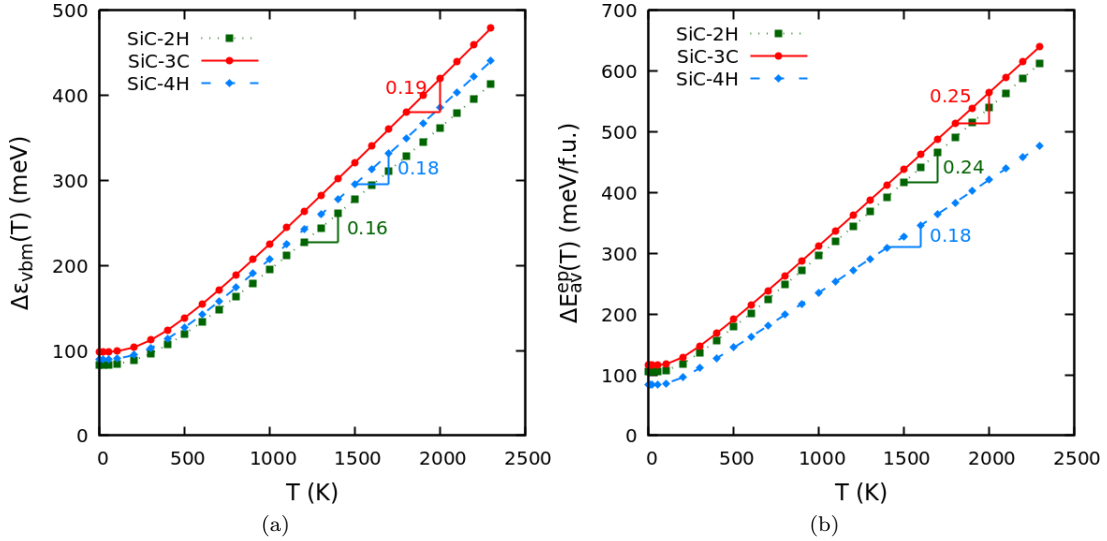


FIG. S6. Finite temperature EPI corrections to (a) VBM and (b) total energy of SiC for DFT lattice parameters for LDA pseudopotential.

Figure S6 shows temperature dependence of the EPI correction to VBM and the total energy for SiC polytypes for pspnc pseudopotential.

The results using pspnc pseudopotential are similar to those from the ONCV pseudopotential presented in the main paper.

Our results from both the GGA.fhi and the pspnc pseudopotentials are similar to those from ONCV pseudopotential. This suggests that the results are stable and independent of the choice of the pseudopotential.

## VI. REFERENCES

- [S1] P. B. Allen, Modern Physics Letters B 34, 2050025 (2020)
- [S2] C. Asker, A. B. Belonoshko, A. S. Mikhaylushkin, and I. A. Abrikosov, Physical Review B 77, 220102 (2008).
- [S3] C. Asker. Effects of disorder in metallic systems from First-Principles calculations. PhD thesis, Linkoping University, Theoretical Physics, The Institute of Technology, 2010.
- [S4] F. Yang, J. Munoz, O. Hellman, L. Mauger, M. Lucas, S. Tracy, M. Stone, D. Abernathy, Y. Xiao, and B. Fultz, Physical Review Letters 117, 076402 (2016).